Short-term depression and long-term plasticity together tune sensitive range of synaptic plasticity

Nicolas Deperrois* and Michael Graupner†

Saints-Pères Paris Institute for the Neurosciences (SPPIN) - CNRS UMR 8003, Université Paris Descartes, 45 rue des Saints Pères, 75270 Paris Cedex 06, France.

February 27, 2019

Abstract

Synaptic efficacy is subjected to activity-dependent changes on short- and long time scales. While short-term changes decay over minutes, long-term modifications last from hours up to a life-time and are thought to constitute the basis of learning and memory. Both plasticity mechanisms have been studied extensively but how their interaction shapes synaptic dynamics is little known. To investigate how both short- and long-term plasticity together control the induction of synaptic depression and potentiation, we used numerical simulations and mathematical analysis of a calcium-based model, where pre- and postsynaptic activity induces calcium transients driving synaptic long-term plasticity. We found that the model implementing known synaptic short-term dynamics in the calcium transients can be successfully fitted to long-term plasticity data obtained in visual- and somatosensory cortex. Interestingly, the impact of spike-timing and firing rate changes on plasticity occurs in the prevalent firing rate range, which is different in both cortical areas considered here. Our findings suggest that short- and long-term plasticity are together tuned to adapt plasticity to area-specific activity statistics such as firing rates.

*current address : Universität Bern, Institut für Physiologie, Bühlplatz 5, CH-3012 Bern, Switzerland.

†To whom correspondence should be addressed at Saints-Pères Paris Institute for the Neurosciences (SPPIN) - CNRS UMR 8003, Université Paris Descartes, 45 rue des Saints Pères, 75270 Paris Cedex 06, France. E-mail, michael.graupner@parisdescartes.fr

Introduction

The impact of presynaptic action potentials on the postsynaptic neuron's excitability varies on multiple time-scales; successive presynaptic spikes produce short-term depression or facilitation lasting for a few minutes, while prolonged pre- and postsynaptic stimulation induce long-term plasticity. How the two interact during activity epochs remains little studied.

Experimental studies in *in vitro* preparations have shown that the induction of synaptic long-term potentiation (LTP) and depression (LTD) depends on (i) the firing rates of pre- and postsynaptic neurons (Dudek and Bear 1992; Sjöström et al. 2001) and on (ii) the precise timing of pre- and postsynaptic action potentials (Markram 1997; Magee 1997; Bi and Poo 1998; Campanac and Debanne 2008). Studies in different brain regions have revealed a marked differences in the dependence of plasticity on spike-timing and frequency (Abbott and Nelson 2000). Furthermore, electrical postsynaptic responses increase and/or decrease upon presynaptic stimulation in a history-dependent manner known as short-term plasticity (STP). A dynamic enhancement of the postsynaptic reponse is termed short-term facilitation and the reduction is called short-term depression (STD). While short-term facilitation has been attributed to the influx of calcium in the presynaptic terminal, short-term depression is attributed to the depletion of some pool of presynaptic vesicles (Zucker and Regehr 2002; Fioravante and Regehr 2011). Different synapses exhibit varied forms of short-term plasticity, being either depression dominated, faciliation dominated, or displaying a mixture of both forms (Markram et al. 1998; Dittman et al. 2000; Wang et al. 2006). Activity-dependent depression dominates synaptic transmission between neocortical pyramidal neurons (Thomson and Deuchars 1994). STP has been proposed as a mechanism serving as dynamic filter for information transmission (see Abbott and Regehr 2004 for a review). A multitude of studies have explored the impact of STP for networks and revealed a variety of computations, such that it may provide a mechanism for working-memory (Mongillo et al. 2008), could be the foundation for interference in cognitive tasks (Kilpatrick 2018), and can improve the mixing capabilities of generative neural networks (Leng et al. 2018), to name a few examples. However, the role of short-term synaptic changes for long-term plasticity induction has attracted little attention.

Plasticity models of different complexities and degrees of biological realism have been developed to capture the link between one or several stimulation protocols that induce long-term plasticity. The classical spike-timing based models capture pair-based spike-time dependent plasticity (STDP; Gerstner et al. 1996; Kempter et al. 1999; Song et al. 2000), but do not account for the firing rate-dependence of plasticity (but see Izhikevich and Desai 2003). To account for the firing-rate dependence and non-linearities of plasticity induction, more complex models have been proposed following phenomenological and biophysical directions (see Morrison et al. 2008 and Graupner and Brunel 2010 for reviews). We here focus on a biophysically inspired model in which both pre- and postsynaptic spike-trains induce postsynaptic calcium elevations which in turn drive plastic changes (Graupner and Brunel 2012; Graupner et al. 2016) as this type of model lends itself easily to incorporate STP.

Similarly, short-term plasticity models have been proposed based on the vesicle depletion model (Liley and North 1953; see Hennig 2013 for a review). This model was later extended by release probability facilitation to account for the mixture of both facilitation and depression present at some synapses (Betz 1970; Varela et al. 1997; Markram et al. 1998; Tsodyks et al. 1998).

Short-term synaptic plasticity has not been considered in the complex models of long-term synaptic plasticity, even though suppression models reducing both pre- and post-synaptic spike efficacies have been proposed to describe the effects of complex spike patters on synaptic modifications (Froemke and Dan 2002; Froemke et al. 2006). Furthermore, the combination of short- and long-term plasticity has been suggested to limit the boundless growth of synapses without weight constraints in a spike-timing based model (Fernando and Yamada 2012).

How do short- and long-term plasticity interact during induction protocols of synaptic long-term changes? Are the brain region and synapse specific realizations of short- and long-term plasticity mechanims related? These questions are pertinent since long-term changes are driven by calcium and calcium transients are affected by short-term dynamics. To address this, we integrate a deterministic model of short-term depression (Abbott 1997; Tsodyks and Markram 1997; Loebel 2009) in the calcium-based model of long-term plasticity (Graupner and Brunel 2012; Graupner et al. 2016). The short-term dynamics parameters account for electrical responses recorded between layer V pyramidal neurons in visual- and somatosensory cortex and are applied to the calcium transients. We fit the calcium-based model including STP to synaptic plasticity data obtained in both brain-regions and we quantify the influence of spike-timing and firing rate changes on the plasticity. We find that short- and long-term plasticity parameters are tuned together such that the sensitive range of synaptic plasticity is located at different firing rate ranges, which match the prevalent firing rates in the respective cortical structures.

Materials and Methods

Calcium-based model of synaptic plasticity

We investigate the calcium-based model where the postsynaptic calcium concentration determines the temporal evolution of the synaptic weight variable, w. The postsynaptic calcium in turn is as a function of pre- and postsynaptic activity. The model is studied extensively in Graupner and Brunel (2012) and Graupner et al. (2016).

Shortly, the postsynaptic calcium concentration drives changes in w according to

$$\tau \dot{w} = \gamma_p (1 - w)\Theta[c(t) - \theta_p] - \gamma_d w \Theta[c(t) - \theta_d]. \tag{1}$$

τ is the time constant of synaptic efficacy changes happening on the order of seconds to minutes. The two terms on the right-hand-side of Eq. (1) describe in a highly simplified fashion calcium-dependent signaling cascades leading to synaptic potentiation and depression, respectively. The synaptic efficacy variable tends to increase, or decrease, when the instantaneous calcium concentration, $c(t)$, is above the potentiation θ_p or the

depression threshold θ_d, respectively (Θ denotes the Heaviside function, $\Theta[c-\theta]=0$ for $c<\theta$ and $\Theta[c-\theta]=1$ for $c\geq\theta$). The parameter γ_p (resp. γ_d) measures the rate of synaptic increase (resp. decrease) when the potentiation (resp. depression) threshold is exceeded.

Here, we consider the evolution of a population of synapses. w therefore describes the *mean* synaptic weight dynamics of a number of synapses forming connections between two neurons. In turn, an activity-dependent noise term appearing in earlier versions of the model (Graupner and Brunel 2012; Graupner et al. 2016) is not considered. In the absence of activity the synapse has a continuum of stable states in Eq. (1). In other words, w is stable at every value $[0,1]$ for $c<\min(\theta_d,\theta_p)$.

Calcium dynamics implementing short-term synaptic depression

The postsynaptic calcium dynamics describes the compound calcium trace resulting from pre- and postsynaptic activity. While contributions from postsynaptic action potentials are assumed to remain constant, calcium increases from presynaptic activity are subject to short-term depression. Note that short-term plasticity has been measured and described with regard to the dynamics of the postsynaptic potential induced by presynaptic stimulation (*e.g.* Loebel 2009). The postsynaptic potential in turn determines the calcium influx through NMDA receptors through the magnesium block, when glutamate is present, and voltage-dependent Ca^{2+} channels (Sabatini et al. 2002). We here assume that postsynaptic voltage is directly proportional to the induced calcium amplitude and use the description of short-term plasticity dynamics in the voltage (Loebel 2009) for calcium.

The average dynamics of short-term synaptic depression can be captured by assuming finite resources. At the event of a presynaptic action potential, a fraction of the resources is utilized to evoke a postsynaptic response. If a subsequent presynaptic action potential arrives before all the utilized resources are recovered, the following postsynaptic response will be smaller (Loebel 2009).

The calcium dynamics is described by

$$\frac{dx}{dt} = \frac{1-x}{\tau_{\mathrm{rec}}} - Ux\sum_i \delta(t-t_i) \tag{2}$$

$$\frac{dc}{dt} = -\frac{c}{\tau_{\mathrm{Ca}}} + C_{\mathrm{pre}}Ux\sum_i \delta(t-t_i-D) + C_{\mathrm{post}}\sum_j (t-t_j), \tag{3}$$

where x denotes the fraction of available presynaptic resources and c is the total calcium concentration. U determines the fraction of the resources utilized at each presynaptic spike, and τ_{rec} is the time constant of resource recovery back to the resting state of $x=1$. τ_{Ca} is the calcium decay time constant. C_{pre} and C_{post} are the pre- and postsynaptically evoked calcium amplitudes, respectively. Note that an isolated presynaptic spike induces a maximal calcium transient of amplitude $C_{\mathrm{pre}}U$ (since all presynaptic resources are available, *i.e.*, $x(t)=1$), and subsequent spikes induce amplitudes of $C_{\mathrm{pre}}Ux$. The sums run over all pre- and postsynaptic spikes occurring at times t_i and t_j respectively. The

time delay, D, between the presynaptic spike and the occurrence of the corresponding postsynaptic calcium transient accounts for the slow rise time of the NMDAR-mediated calcium influx. Without loss of generality, we set the resting calcium concentration to zero, and use dimensionless calcium concentrations.

The parameters describing short-term depression in somatosensory cortex are $U = 0.46$ and $\tau_{\text{rec}} = 525$ ms (Loebel 2009). Using the same approach as described in Loebel (2009), we adapted the short-term depression model (Eqs. (2) and (3)) to voltage traces recorded between L5 neurons of visual cortex. (Fig. 1C in Sjöström et al. 2003). Utilizing a least squares fitting routine, we obtained $U = 0.385$ and $\tau_{\text{rec}} = 149$ ms (see Tab. 1 and Fig. 1A).

For comparison, we also study the calcium-based plasticity model *without* short-term depression. In this case, the presynaptically evoked calcium amplitude is C_{pre} in response to *all* presynaptic spikes. The calcium dynamics simplifies to

$$\frac{dc}{dt} = -\frac{c}{\tau_{\text{Ca}}} + C_{\text{pre}} \sum_i \delta(t - t_i - D) + C_{\text{post}} \sum_j (t - t_j). \tag{4}$$

Fitting the plasticity models to experimental data

In order to compare plasticity between visual- and somatosensory cortex, we fitted the calcium-based plasticity model with the corresponding short-term depression parameters and without short-term depression to experimental plasticity data obtained from synapses between layer V neurons in the rat visual cortex (Sjöström et al. 2001) and between layer V neurons in the rat somatosensory cortex (Markram 1997). Note that the short-term depression parameters were not optimized during the fit to the long-term plasticity data but kept fixed (see previous paragraph).

The stimulation protocols employed in visual- (Sjöström et al. 2001) and in somatosensory cortex (Markram 1997) combine spike-timing and firing rate components by varying the presentation frequency of spike-pairs with constant time lag, Δt. Stimulation patterns are grouped in five pairs of pre- and postsynaptic spikes with long pauses in between in order to allow for full recovery of short-term depression processes between each group of five pairs. Specifically, Sjöström et al. (2001) repeated the bursts of five pre- and postsynaptic spikes 15 times every 10 s, while Markram (1997) repeated the bursts 10 times every 4 s. The time lag between pre- and postsynaptic spikes as well as the presentation frequency of the pairs within the burst were systematically varied in both studies (see experimental data in Fig. 2A).

We consider the change in synaptic strength as the ratio between the synaptic strength after and before the stimulation protocol $w(T)/w_0$, where T marks the end of the stimulation protocol. $w_0 = 0.5$ in all simulations and calculations. As a consequence, the maximally evoked change remains in the interval $[0, 2]$.

We defined the goodness of fit to the experimental plasticity data by a cost function which is the sum of all squared differences (SSD : sum of squared differences) between data points and the analytical solution for the change in synaptic strength of the calcium-based model. We drew initial parameter values from a uniform distribution and use a

downhill Simplex algorithm to search the minimum of the cost function. The fit is repeated $> 10^9$ times and the parameter set with the lowest cost function is used (shown in Tab. 1).

plasticity type	parameter	unit	visual ctx.		somatosens. ctx.	
short-term	U		0.3838	-	0.46	-
	τ_{rec}	ms	148.9192	-	525	-
long-term	τ_{Ca}	ms	39.6511	33.0576	55.5959	43.4916
	C_{pre}		1.9955	0.7724	0.6893	0.7609
	C_{post}		0.9827	1.0	1.0753	0.5404
	θ_d		**1**	**1**	**1**	**1**
	θ_p		1.5343	1.5892	**1.2**	**1.2**
	γ_d		179.9331	161.3423	45.2551	102.9918
	γ_p		923.4246	820.9043	139.3637	343.2946
	τ_{cb}	sec	405.0252	312.6557	17.9134	22.4382
	D	ms	10	10	5.3437	5.4418
fit quality	**SSD**		**0.05637**	**0.02156**	**0.01079**	**0.002550**

Table 1: Parameters for short-term and long-term plasticity in visual- and somatosensory cortex. The short-term plasticity parameters shown in the first two lines are obtain from fitting the STD model to visual cortex voltage traces (left column, Fig. 1C in Sjöström et al. 2003), and are taken from Loebel (2009) for the somatosensory cortex (right column). Long-term plasticity parameters are obtained by fitting the calcium-based model with short-term depression to visual- (Sjöström et al. 2001) and somatosensory cortex plasticity data (Markram 1997). Values in bold were not allowed to be optimized by the fitting routine. The last line give the SSD for all four cases providing a measure of the fit quality.

Irregular spike-pair stimulation

To study changes in synaptic efficacy induced by firing rate and spike correlations under more natural conditions, we use irregular spike-pair stimulation. This stimulation protocol was proposed and extensively studied in Graupner et al. (2016). In short, irregular spike-pairs were generated using discretely correlated Poisson processes. The presynaptic neuron emitted spikes with Poisson statistics at rate ν_{pre}. Each of these presynaptic spikes induced with probability p a postsynaptic spike with a fixed time lag Δt. The postsynaptic neuron in addition emits independent spikes with Poisson statistics at a rate $\nu_{\mathrm{post}} - p\nu_{\mathrm{pre}}$, so that the total postsynaptic firing rate is ν_{post}.

We systematically varied the firing rates with $\nu_{\mathrm{pre}} = \nu_{\mathrm{post}}$, Δt and p. p effectively controls the strength of spiking correlation between pre- and postsynaptic neuron, with maximal correlation for $p = 1$ (each presynaptic spike is followed by a postsynaptic one) and independent Poisson firing for $p = 0$. The stimulation is imposed for a duration of $T = 10$ s, independently of the firing rate (so that the total number of emitted spikes varies with the firing rate).

To quantitatively compare the influence of firing rates and spike correlations on synaptic changes in irregularly firing neurons, we quantify the sensitivity of synaptic strength to correlations and firing rate changes (Graupner et al. 2016). These measures give the change in synaptic weight when adding spike correlations to uncorrelated pre- and

postsynaptic neurons, or when increasing the firing rate by a certain amount. In short, the synaptic efficacy $w(T)$ at the end of a stimulation protocol of duration T is a random variable, the value of which depends on the precise realization of the pre- and postsynaptic spike trains, their firing rates and their correlation. The average synaptic efficacy $\bar{w}(T)$ can be written as

$$\bar{w}(T) = \bar{w}_{\text{no corr}}(\nu_{pre}, \nu_{post}, T) + \bar{w}_{\text{corr}}(\nu_{pre}, \nu_{post}, C(t), T), \tag{5}$$

where $\bar{w}_{\text{no corr}}$ is the average synaptic efficacy attained for uncorrelated pre- and postsynaptic spike trains of rates ν_{pre} and ν_{post}. The quantity $\bar{w}_{\text{corr}}$ represents the additional change in synaptic efficacy induced by correlations between the pre- and postsynaptic spike trains. We call $\bar{w}_{\text{corr}}$ the *sensitivity of synaptic strength to correlations*. Note that this sensitivity to correlations depends both on the correlation function $C(t)$ between the pre- and postsynaptic spike trains and individual firing rates of the neurons.

We compare the sensitivity of synaptic strength to correlations to the sensitivity to firing rates $\delta\bar{w}_{\text{no corr}}$, defined as the change between the synaptic strength attained at a given, baseline pre- and postsynaptic firing rate, and the synaptic strength attained by increasing the firing rates by a given amount $\delta\nu$:

$$\delta\bar{w}_{\text{no corr}}(\nu_{pre}, \nu_{post}, \delta\nu) = \bar{w}_{\text{no corr}}(\nu_{pre} + \delta\nu, \nu_{post} + \delta\nu, T) - \bar{w}_{\text{no corr}}(\nu_{pre}, \nu_{post}, T). \tag{6}$$

Note that this sensitivity depends both on the baseline firing rates ν_{pre}, ν_{post}, and the amount of increase in the firing rates $\delta\nu$.

Results

To study the interplay between short-term- and long-term plasticity, we used numerical simulations and mathematical analysis of a calcium-based plasticity model (Graupner and Brunel 2010; Graupner et al. 2016). We first extracted synaptic short-term depression dynamics for the respective cortical region from voltage recordings and used these to describe calcium transient dynamics. We then fitted the plasticity model to plasticity results obtained in the visual cortex (Sjöström et al. 2001) and the somatosensory cortex (Markram 1997). Finally, we studied how firing rate and spike-timing shape plasticity in both cortical areas with irregular activity patterns.

Short-term depression strongly affects the calcium trace during bursts of activity

In order to study the interplay between short-term depression (STD) and long-term plasticity, we first extracted the short-term depression dynamics of EPSP amplitudes for visual- and somatosensory cortex. Assuming that the influence of STD on the calcium flux through NMDA receptors and voltage-dependent Ca^{2+} channels is linear (see Methods), we applied the same amplitude dynamics to calcium amplitudes elicited by bursts of presynaptic activity.

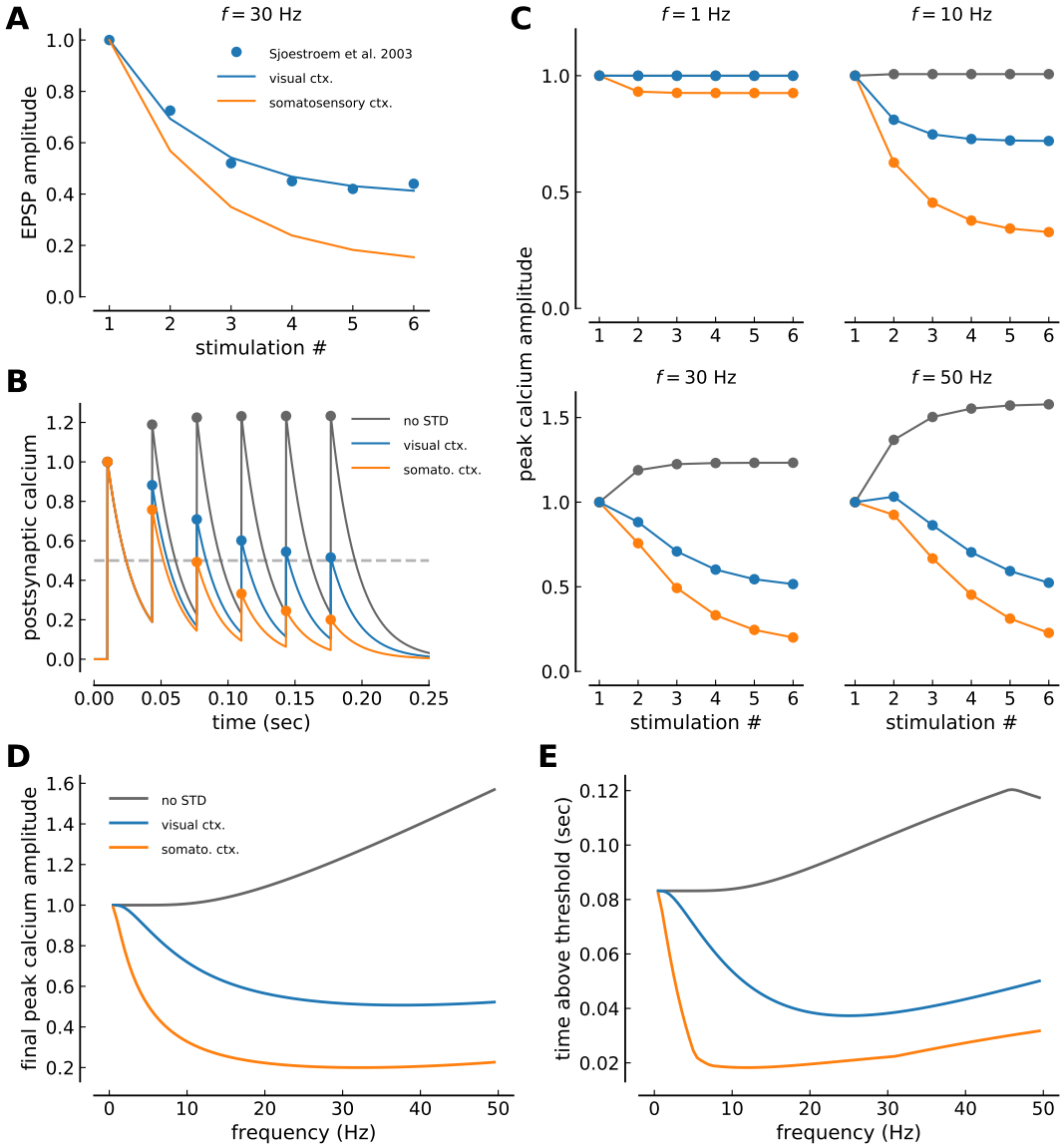

Figure 1: Calcium dynamics with short-term depression in visual and somatosensory cortex. ***(A)*** Experimental data of relative EPSP amplitudes in response to a train of six action potentials at 30 Hz in visual- (blue) and somatosensory cortex (orange). The points show data from visual cortex (Fig. 1C in Sjöström et al. 2003). The lines show the description through the short-term depression model (Eqs. (2),(3)). ***(B)*** Example calcium traces with visual cortex STD (blue), somatosensory cortex STD (orange) and no STD (gray line). Traces are generated by six presynaptic stimuli occurring at 30 Hz. Peak calcium amplitudes upon each stimulation are marked by circles. ***(C)*** Peak calcium amplitudes in response to a train of six stimuli at various frequencies (marked on top of each panel). Peak amplitudes of the calcium trace (see panel *D*) at the time of the stimulation are shown for visual cortex STD (blue), somatosensory cortex STD (orange) and no STD (gray line). ***(D)*** Final peak calcium amplitude at the sixth presynaptic stimuli as function of stimulation frequency for visual cortex STD (blue), somatosensory cortex STD (orange) and no STD (gray line). The plotted peak corresponds to the last point in panel *C*. ***(E)*** Time spent above threshold by the calcium trace during the train of six presynaptic stimuli as function of stimulation frequency. For illustration, a threshold of $\theta = 0.5$ is used. Color code as in panel *D*. An initial calcium amplitude of 1 is used for all cases and the calcium decay time constant is taken to be $\tau_{\mathrm{Ca}} = 20$ ms in *B*-*E*.

We use a deterministic model of STD which describes the average temporal dynamics of the postsynaptic calcium responses to presynaptic stimulation (see Methods, Eqs. (2), (3)). STD has been characterized for connections betwen L5 pyramidal neurons in the somatosensory cortex (Loebel 2009). We fitted the deterministic model to EPSP responses obtained between L5 neurons in visual cortex (Sjöström et al. 2003, Fig. 1*A*, see parameters in Tab. 1). Comparing both parameter sets reveals differences betweeen visual and somatosensory cortex STD. More presynaptic resources are utilized in somatosensory cortex upon stimulation (*i.e.*, $U_{\text{vis. ctx.}} < U_{\text{somat. ctx}}$), and the recovery time of these resources is longer in somatosensory cortex (see Tab. 1 and Fig. 1).

STD dynamics applied to calcium drastically alters the postsynaptic calcium response upon repeated presynaptic stimulation. While calcium transients build up and reach a plateau of attained amplitudes without STD (see gray lines in Fig.1*C*), subsequent calcium transients decrease with STD and this difference increases with frequency (see Fig.1*C* 50 Hz case). Irrespective of responses in visual or somatosensory cortex, the decrease in induced calcium amplitudes due to STD prevents the calcium trace from exceeding the amplitude of the first transient up to high stimulation frequencies ($f < 46$ Hz for visual cortex; $f < 62$ Hz for somatosensory cortex). In turn, no plateau is reached and the transients keep decreasing for consecutive stimulations.

Overall, postsynaptic responses to repeated presynaptic stimulation are suppressed stronger in the somatosensory cortex compared to the visual cortex since the fraction of used resources, U, is larger in the somatosensory cortex (Tab. 1, Fig. 1*D,E*). Moreover, the depression happens already at low (< 5 Hz) frequencies since the recovery time constant of presynaptic resources is longer in the somatosensory cortex compared to the visual cortex (Fig. 1, Tab. 1). As a consequence, the calcium amplitude (Fig. 1*D*) and the time spent by the calcium trace above a given threshold (Fig. 1*E*) change drastically in the frequency range up to 5 Hz in the somatosensory cortex, while the change occurs for a larger frequency range in the visual cortex.

In summary, the differences in STD lead to a strong suppression of postsynaptic responses at low frequencies in the somatosensory cortex while the same suppression occurs over a larger frequency range in the visual cortex.

Calcium-based model with STD fitted to experimental plasticity data

Plasticity is driven by postsynaptic calcium elevations which is captured by the calcium-based plasticity model, where threshold crossings drive long-term depression and potentiation processes. STD on the other hand leads to a highly dynamics calcium trace with changing amplitudes upon each stimulation and furthermore prevents considerable build-up of calcium even at relatively high presynaptic stimulation frequencies (Fig. 1). Here we ask whether the calcium-based plasticity model with STD can capture the experimental plasticity data obtained by combining spike-timing and frequency stimulation.

Pre- and postsynaptic spikes with delay Δt presented in bursts of five pairs at varying frequencies has been shown to induce LTP for pre-post spike-pairs ($\Delta t = 10$ ms) for frequencies ≥ 10 Hz in visual- and somatosensory cortices. Post-pre pairs ($\Delta t = -10$ ms) evoke LTD at low frequencies in both structures (< 30 Hz) and LTP at high frequencies

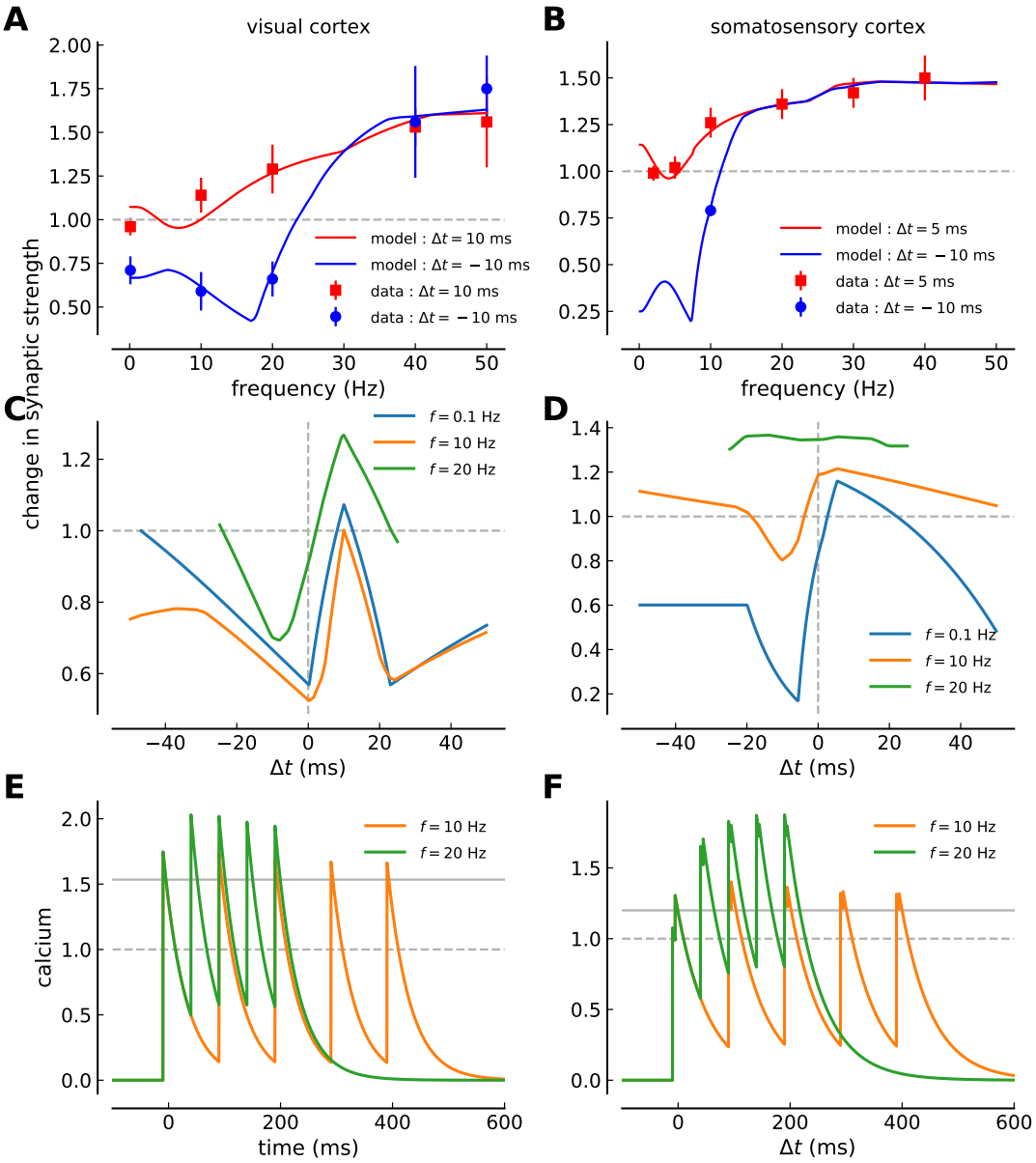

Figure 2: Calcium-based plasticity model with short-term depression fitted to visual- and somatosensory cortex plasticity data. ***(A, B)*** The change of the synaptic strength is shown as a function of the spike-pair presentation frequency for regular pre-post pairs ($\Delta t = 10$ ms in A and $\Delta t = 5$ ms in B, red squares and lines), and regular post-pre pairs ($\Delta t = -10$ ms in both panels, blue circles and lines). The data-points are taken from plasticity experiments in visual cortex slices (A, mean $\pm$ SEM, Sjöström et al. 2001) and somatosensory cortex slices (B, mean $\pm$ SEM, Markram 1997). The solid lines show the model fit to the experimental data. ***(C, D)*** Change in synaptic strength as a function of the time lag between pre-and postsynaptic spikes for regular spike-pairs at three different spike-pair presentation frequencies (given in panel) in visual- (C) and somatosensory cortex (D). ***(E, F)*** Calcium traces during regular post-pre spike-pair stimulation for the visual- (E) and somatosensory data-set (F). Five spike-pairs with $\Delta t = -10$ ms are presented at the frequency given in the panel. The full and the dashed gray lines indicate the area-specific thresholds for potentiation and depression, respectively.

in the visual cortex (Fig. 2*A,B*).

The postsynaptic response to spike-pairs presented in bursts is subjected to STD. We therefore implemented STD dynamics in the calcium driving the plasticity changes in the model and fitted the long-term plasticity model parameters to plasticity data obtained in visual- and somatosensory cortices. The parameters describing the STD dynamics are specific for each cortical region considered and are kept constant during that fit (see Tab. 1).

We find that the calcium-based plasticity model with STD of the calcium dynamics captures the experimental data of visual- and somatosensory cortex (Fig. 2*A,B*). In particular, the model retains the frequency dependence of plasticity for both, pre-post and post-pre pairs despite the strong frequency-dependent suppression of presynaptically evoked calcium amplitudes. The fit of the calcium-based model yields STDP curves which are dominated by depression for low pair presentation frequencies (Fig. 2*C,D*). Intermediate frequencies yield curves with depression for $\Delta t < 0$ ms and potentiation for $\Delta t > 0$ ms, whereby intermediate frequencies implies $f \approx 20$ Hz in visual cortex and $f \approx 10$ Hz in somatosensory cortex.

Due to STD, we find a non-monotonic behavior of LTD *and* LTP with respect to the stimulation frequency. The model predicts weak LTP for very low presentation frequencies of pre-post ($\Delta t = 10$ ms) pairs (Fig. 2*A,B*). This LTP vanishes at frequencies around 5 Hz and re-emerges at higher rates, a behavior which is due to STD-induced reduction in presynaptically evoked calcium and not seen in the model variant without STD (see Fig. 5*A,B*). Not LTP but no change has been measured in visual cortex at 0.1 Hz where the sparse data points hint to a monotonic increase of LTP (Fig. 2*A*). Such low stimulation frequencies were not investigated in somatosensory cortex (Fig. 2*B*).

Two particular features of somatosensory plasticity stand out : (i) the rapid transition from LTD to LTP for post-pre pairs ($\Delta t = -10$ ms) between 8 and 15 Hz, (ii) and loss of distinction between pre-post and post-pre pair induced plasticity at ~ 14 Hz. In contrast for the visual cortex, LTD is induced for post-pre ($\Delta t = -10$ ms) stimulation from 0.1 up to about 25 Hz and the difference between pre-post and post-pre stimulation vanishes at 30 Hz stimulation. Comparing these frequencies indicates that the range of different plasticity results for pre-post and post-pre stimulation is restricted to lower frequencies in the somatosensory- compared to the visual cortex.

The calcium traces for 10 and 20 Hz regular spike-pair stimulation in both structures (Fig. 2*E,F*) demonstrate the two factors responsible for the rapid transition from LTD to LTP in somatosensory cortex : (i) The difference between depression and potentiation threshold is small such that the LTP threshold is crossed and LTP is induced as soon as the calcium trace starts to accumulate for increasing frequencies ($\theta_d = 1$, $\theta_p = 1.2$ in somatosensory ctx.; $\theta_d = 1$, $\theta_p = 1.5343$ in visual ctx.). (ii) The calcium decay time constant, τ_{Ca}, is such that consecutive calcium transients start to accumulate between 10 and 20 Hz stimulation ($\tau_{\mathrm{Ca}} = 55.6$ ms for somatosensory and 39.7 ms for visual cortex; see Tab. 1). In the visual cortex, the difference between both thresholds is larger and the calcium decay time constant is faster (see Tab. 1). As a result, 10 *and* 20 Hz stimulation dominantly activate depression leading to LTD for both cases.

Calcium responses to presynaptic stimulation suppress stronger in the somatosensory

cortex (see Fig. 1). In turn, any difference in the calcium trace between pre-post and post-pre stimulation disappears at lower stimulation frequencies in the somatosensory- compared to the visual cortex. This fact explains why the distinction in induced plasticity between pre-post and post-pre stimulation disappears at low stimulation frequencies in the somatosensory cortex. In other words, if the calcium traces for $\Delta t = -10$ ms and $+10$ ms are alike, the times spent above potentiation and depression thresholds and therefore the induced plasticity are identical. This becomes furthermore apparent in the fit of the model variant without STD to the somatosensory plasticity data. Here, the difference in induced plasticity for pre-post vs. post-pre pairs is retained for frequencies up to ~ 30 Hz (see Fig. 5*B*).

In summary, the spike-timing- and frequency dependence of synaptic plasticity can be captured by the calcium-based model endowed with STD dynamics in the calcium. In particular, the model resolves the experimentally measured difference between pre-post and post-pre spike-pair stimulation.

Irregular spike-pair presentations strongly reduces the impact of spike-timing on synaptic plasticity

Spike-pairs in the plasticity experiments considered above were presented in a regular fashion, that is, with fixed inter-pair intervals. In a step towards more natural, irregular firing patterns, we use the previously suggested protocol of Poisson-distributed spike-pairs (Graupner et al. 2016), where the presynaptic neurons fire spikes according to a Poisson process but each spike is followed by a postsynaptic spike at time lag Δt which probability p.

A simple shift from regular pre- and postsynaptic spike-pairs to spike-pairs with the same timing constraints but irregular distribution has a strong impact on STDP curves (Fig. 3). At all frequencies, the change in synaptic strength is dominated by LTP, while the LTD part of the curves is strongly reduced or even disappears for plasticity in the visual cortex (Fig. 3*A*). Strikingly, the range of plasticity values obtained when varying the time lag between pre- and postsynaptic spikes, Δt, is much reduced for irregular spike pairs.

Irregular presentation of spike-pairs strongly reduced the impact of spike-timing on synaptic changes, as previously noted (Graupner et al. 2016). This effect still holds true when STD is present in the calcium dynamics.

Synaptic changes occur at very different firing rate ranges across cortices

Lastly, we studied how synaptic changes in response to firing rate increases compare with changes from correlations and ask in particular in which firing rate range plasticity is most sensitive to both changes.

In visual- and somatosensory cortex, when increasing the uncorrelated firing rate in pre- and postsynaptic neurons, the change in synaptic strength follows a BCM-type of curve (Bienenstock et al. 1982): no change when both neurons are inactive, depression at low rates and potentiation at intermediate to high firing rates.

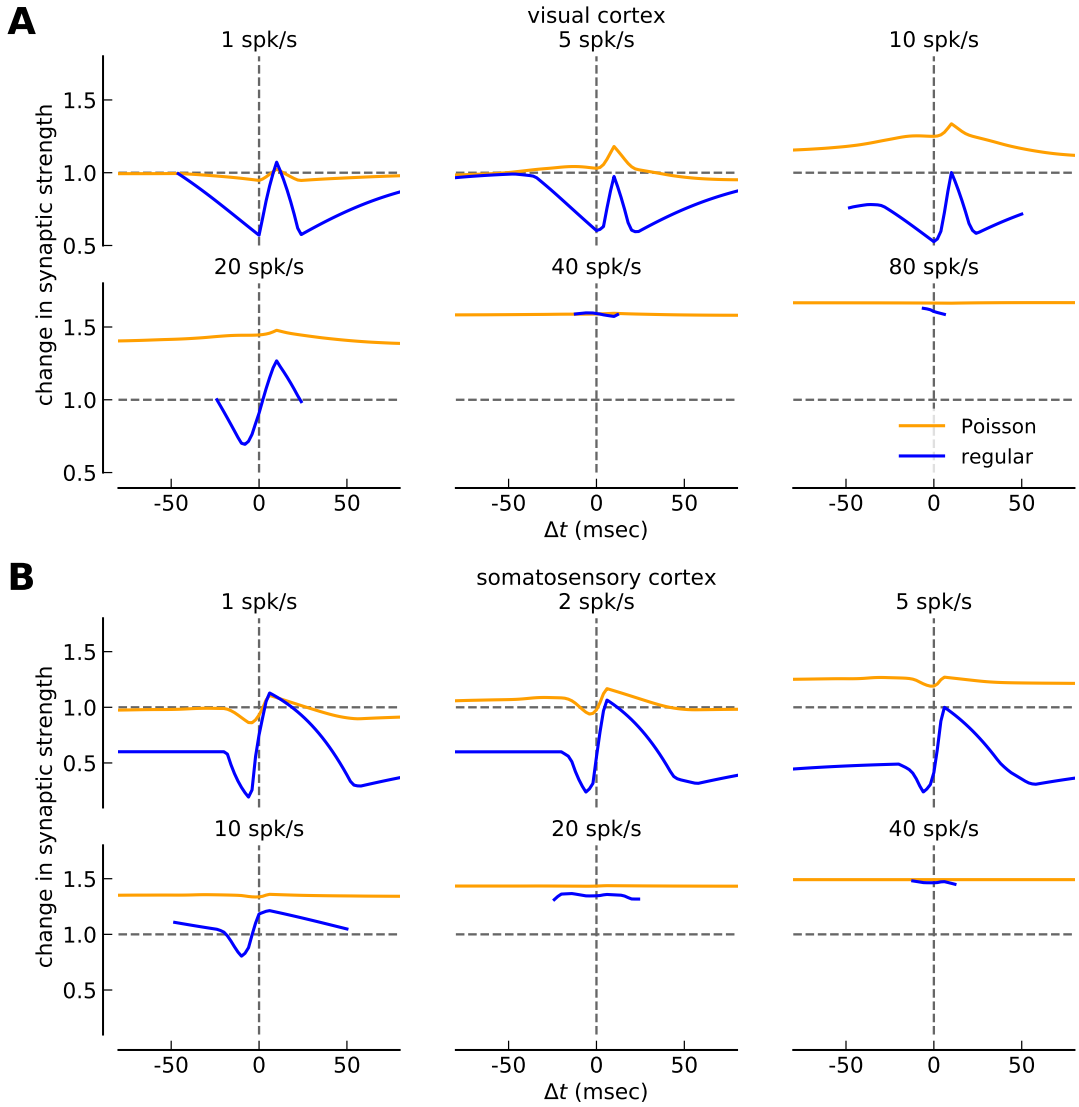

Figure 3: Change in synaptic strength in response to irregular and regular spike-pairs at different firing rates. ***(A, B)*** Change in synaptic strength as a function of the time lag between pre- and postsynaptic spikes for irregular (orange) and regular spike-pairs (blue) at different firing rates for the calcium-based plasticity model with STD dynamics of the calcium. The STDP curves for the visual cortex parameter-set is shown in A while somatosensory examples are shown in B. Note that all synaptic changes are shown from a 10 s stimulation and with $p = 1$, *i.e.*, the number of spikes occurring during a stimulation protocol varies with the firing rate and each presynaptic spike is followed or preceded by a postsynaptic one at time lag Δt. Note that the curves for regular spike-pairs are shown for the interval $\Delta t \in [-1/(2\nu), 1/(2\nu)]$ only as the same curve is repeated for larger values of Δt.

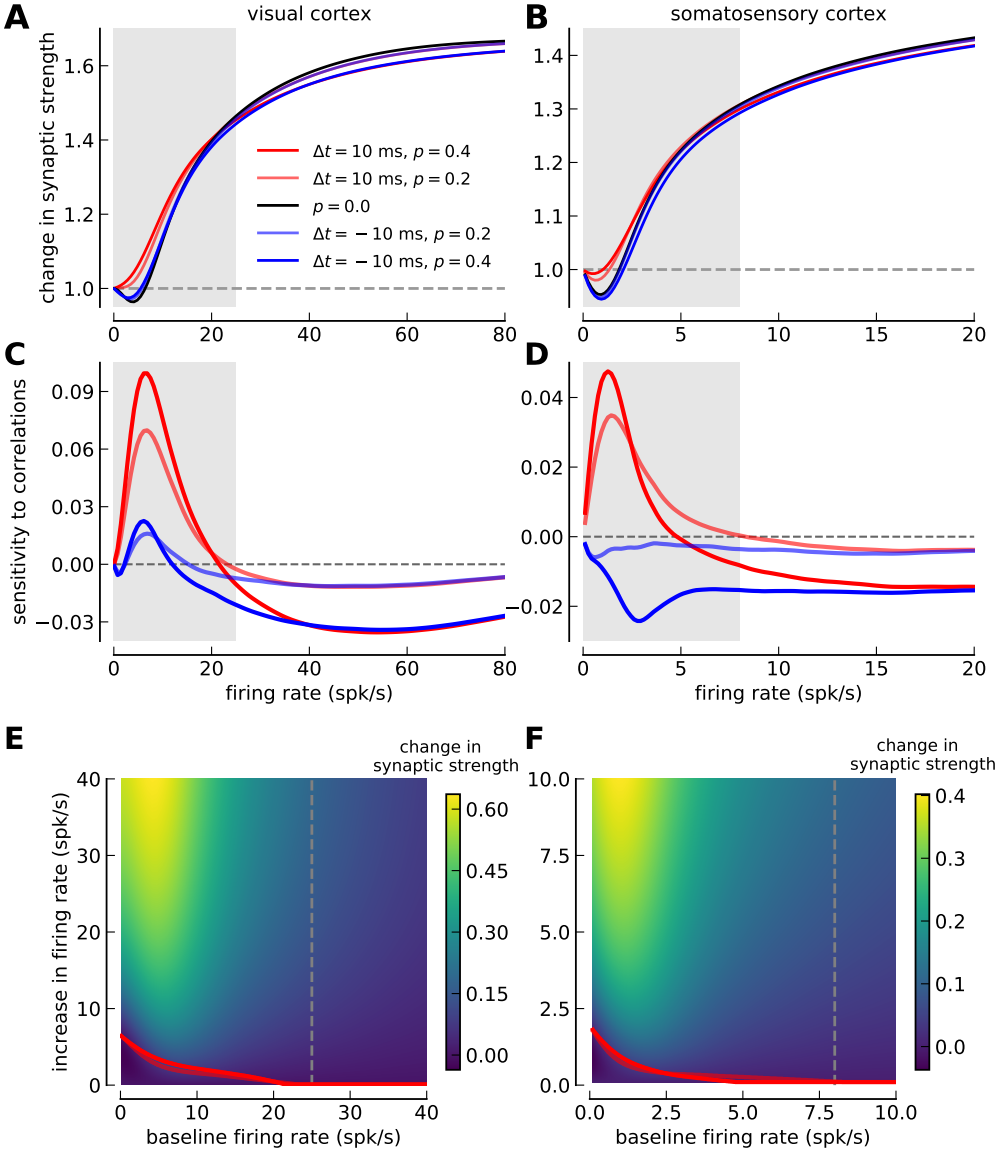

Figure 4: Comparing the sensitivity of synaptic plasticity to firing rate and spike-timing between visual- and somatosensory cortex. ***(A, B)*** Change in synaptic strength as a function of the firing rate for several values of the correlation coefficient p and time lag Δt in visual- (A) and somatosensory cortex (B). Five cases are shown : (i) uncorrelated Poisson spike trains (black), (ii) pre-post pairs with $\Delta = 10$ ms at $p = 0.2$ (light red) and $p = 0.4$ (dark red); and (iii) post-pre pairs with $\Delta = -10$ ms at $p = 0.2$ (light blue) and $p = 0.4$ (dark blue). ***(C, D)*** Sensitivity of synaptic changes to spike-pair correlations (see Methods, Eq. (5)) in visual- (C) and somatosensory cortex (D). The change in synaptic strength due to spike-timing correlations is shown as a function of the firing rate. ***(E, F)*** Sensitivity of synaptic changes to firing rate changes (see Methods, Eq. (6)) in visual- (C) and somatosensory cortex (D). Color plots represent the synaptic change as a function of the baseline firing rate (x-axis) and the increase in firing rate (y-axis). Light and dark red lines indicate the firing rate increase evoking the same synaptic change as spike-pair correlations at $\Delta t = 10$ ms with $p = 0.2$ and $p = 0.4$, respectively. Prevalent firing rate ranges in visual (< 25 spk/s; Livingstone and Hubel 1981) and somatosensory cortex (< 8 spk/s; Crochet and Petersen 2006) are marked by gray shaded regions in panels A-D and by a gray, dashed line in panels E,F. Note the different firing rate ranges shown on the x-axis between the left and the right column. All changes are in response to a stimulation for 10 s.

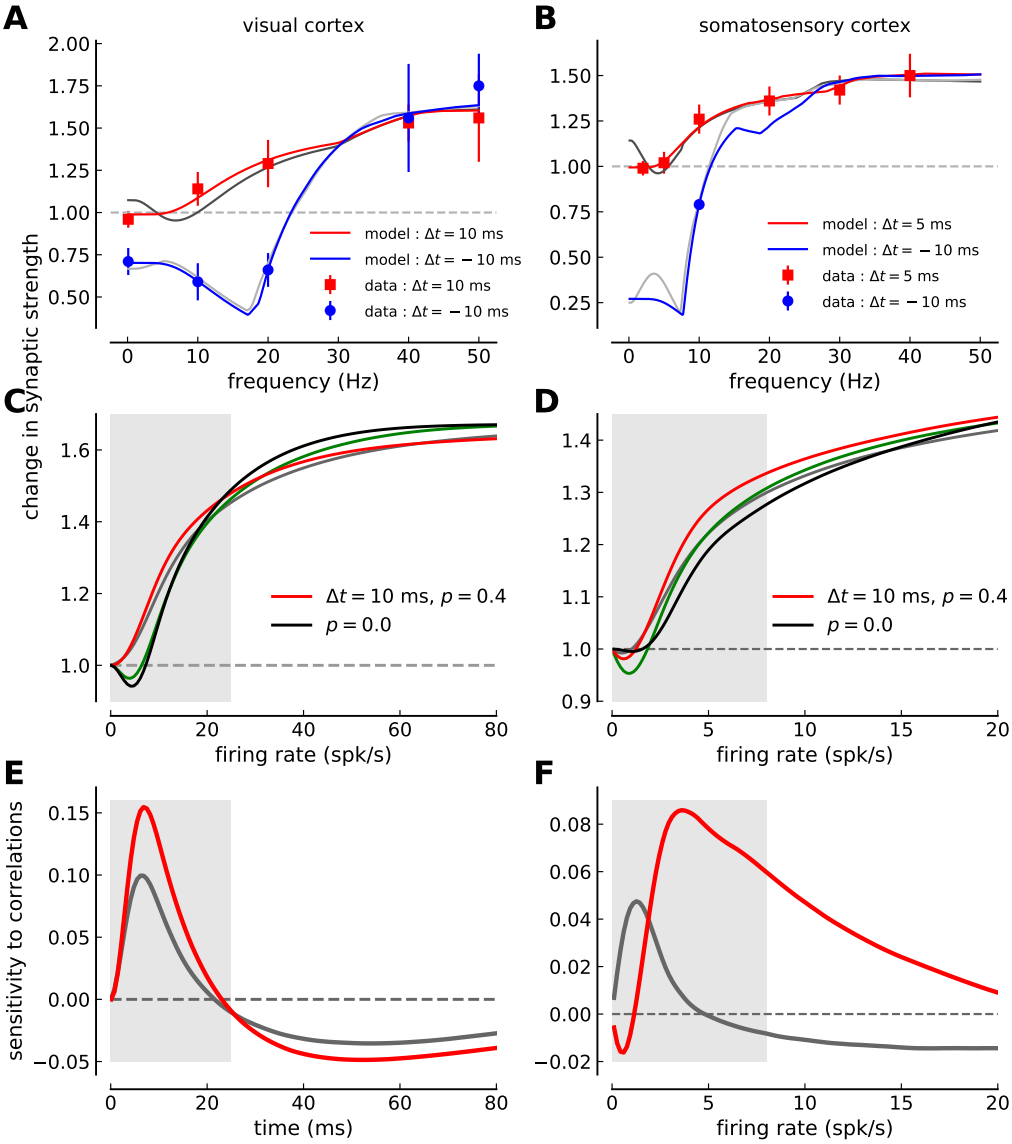

Figure 5: Comparison between model versions with and without short-term depression. ***(A, B)*** Model fit (solid lines) to the experimental plasticity data obtained in visual cortex (A, mean ± SEM, Sjöström et al. 2001) and somatosensory cortex slices (B, mean ± SEM, Markram 1997). Same depiction as in Fig. 2. The red and blue lines show the model without STD fitted to the data, while the gray lines are a reproduction from Fig. 2A,B of the model with STD. ***(C, D)*** Change in synaptic strength in response to irregular pre- and post activity as a function of the firing rate for several values of the correlation coefficient p and one time lag Δt in visual- (C) and somatosensory cortex (D). Two cases are shown for the model without STD : (i) uncorrelated Poisson spike trains ($p = 0$, black) and (ii) pre-post pairs with $\Delta = 10$ ms at $p = 0.4$ (red). These two cases are also shown for the model with STD : (i) uncorrelated Poisson spike trains shown in green, and (ii) pre-post pairs with $\Delta = 10$ ms at $p = 0.4$ shown in gray. ***(E, F)*** Sensitivity of synaptic changes to spike-pair correlations in visual- (E) and somatosensory cortex (F). The change in synaptic strength due to spike-timing correlations is shown as a function of the firing rate for the model without STD (red) and with STD (gray; same line as in Fig. 4C,D). Prevalent firing rate ranges in visual (< 25 spk/s; Livingstone and Hubel 1981) and somatosensory cortex (< 8 spk/s; Crochet and Petersen 2006) are marked by gray shaded regions in panels C-F. Note the different firing rate ranges shown on the x-axis between the left and the right column of panels C-F. All changes in panels C-F are in response to a stimulation for 10 s.

Adding pre-post correlations ($\Delta t > 0$ ms) increases the change in synaptic strength at low firing rates (*i.e.* < 25 spk/s in visual cortex and < 8 spk/s in somatosensory cortex; Fig. 4*C,D*). Post-pre correlations entail little change compared to uncorrelated pre- and postsynaptic activity (see blue lines in Fig. 4*C,D*).

Even though the qualitative plasticity behavior is very similar between visual- and somatosensory cortex, that is, the sensitivity to firing rate and correlations exhibits the same overall behavior, the synaptic changes occur in very different firing rate ranges. Synaptic plasticity is most sensitive to changes in firing rate and correlations for rates up to ~ 15 spk/s in the visual cortex, while the same amplitudes of sensitivities extends only up to ~ 5 spk/s in the somatosensory cortex (Fig. 4). In other words, changes due to activity alterations are induced at much lower firing rates in the somatosensory cortex compared to the visual cortex. Similarly to the difference in the sensitive ranges of plasticity, the prevalent firing rates in the visual- and somatosensory cortex are very different : while neurons in the visual cortex *in vivo* reach activities up to 25 spk/s (Livingstone and Hubel 1981), they fire up to 8 spk/s in the somatosensory cortex *in vivo* (Crochet and Petersen 2006) (see gray shaded regions in Fig. 4).

Where does this difference in sensitive ranges between somatosensory- and visual cortex come from? As discussed above, the rapid transition from LTD to LTP in the somatosensory cortex emerges from the short extend of the LTD region, that is, the small difference between depression and potentiation thresholds (see Tab. 1). This difference is larger in the visual cortex which in turn gives rise to a slower transition to maximal LTP upon firing rate increases. The dissimilar sensitivities to firing rate changes between visual- and somatosensory cortex are the result of this difference in potentiation thresholds.

Comparing model variants with and without STD fitted to the experimental data (Fig. 5) illustrates that STD in the somatosensory cortex is responsible for restricting the correlation sensitivity to low firing rates < 5 spk/s. The somatosensory model variant without STD exhibits sensitivity to correlations up to ~ 20 spk/s which goes well beyond the prevalent firing rates in that region (see Fig. 5*F*). With STD and as outlined above, the stronger suppression of presynaptically evoked calcium traces in the somatosensory cortex as compared to the visual cortex explains the disappearance of correlation sensitivity at low firing rates.

In summary, there is a perfect match between the predominant firing rates and the sensitive ranges of the synaptic plasticity in visual- and somatosensory cortex. Synaptic long- and short-term plasticity are tuned such that LTD and LTP occur at realistic firing rate ranges in both cortices.

Discussion

Using numerical simulations, we have explored the impact of short-term depression on long-term plasticity induction in visual- and somatosensory cortices. We fitted the calcium-based plasticity model to spike-pair- and frequency plasticity data in both structures and showed that the experimental data can be captured despite the activity-

dependent reduction in presynaptically induced calcium transients during the burst stimulation. When examining plasticity in response to more *in vivo*-like, irregular stimulation patterns, we show that short-term and long-term plasticity parameters ensure that synaptic changes are susceptible to rate and correlation changes within the prevalent firing rates in both cortical areas, which are markedly different. Our findings suggest that long- and short-term synaptic plasticity are together tuned to account in combination for the activity properties of the synapse's location.

Long-term plasticity alters and short-term plasticity dynamics

The induction of long-term plasticity is known to alter the short-term plasticity due to the presynaptic expression of the long-term changes (Sjöström et al. 2003). LTD induction, for example, reduces short-term depression due to a reduction in transmitter release. Here we use short-term plasticity parameters fitted to baseline responses between layer V pyramidal cells, that is, before long-term plasticity induction. This approach is justified as there is a clear separation of time scales, LTD/LTP induction protocols last for a few minutes : 2.5 min in visual cortex (Sjöström et al. 2001) and 40 s in somatosensory cortex (Markram 1997) while the expression of long-term changes builds up over the course of tens of minutes (Sjöström et al. 2003).

Stochastic vesicle release

The deterministic short-term plasticity model utilized here is fitted to average postsynaptic responses. However, transmitter release is a stochastic process and as a consequence the magnitude of the postsynaptic response evoked by each presynaptic action potential fluctuates, even with the same preceeding activity pattern. The quantal nature of synaptic transmission is described by binomial statistics (Zucker and Regehr 2002; Loebel 2009). In turn, stochastic synaptic short-term plasticity parameters not only describe the change in the average response, but also the magnitude of fluctuations of individual responses. The variability of calcium responses impacts the induction of long-term plasticity in protocols repeating the same stimulation pattern multiple times (10 to 15 times as used here). Whether experimental plasticity data can be captured under such conditions and how stochastictiy affects firing rate and correlation sensitivities is the subject of future research.

Validity of the results in vivo

Long-term plasticity in slices has been induced with elevated extracellular calcium concentrations while *in vivo* calcium levels are estimated to be around 1.5 mM (Silver 1990). Considering realistic calcium levels will most likely change the plasticity rules observed *in vitro* under elevated extracellular calcium (Higgins et al. 2014) and has to be considered when applying our results to *in vivo* data. Most of the data on short-term plasticity stems from brain slices but a recent study established STD to be involved in the adaptation to sensory responses in the somatosensory cortex *in vivo* (Chung et al. 2002).

Generality of model results

The deterministic short-term depression model utilized here has been fitted to evoked voltage responses between layer V neurons in somatosensory- and visual cortex. The two parameter sets describing STD dynamics are well constrained by these traces and provide a reliable account of the mean postsynaptic response, which is used for the calcium dynamics description here. Conversely, the calcium-based long-term plasticity model (7 or 8 free parameters) is insufficiently constrained by the 10 and 7 LTP/LTD datapoints from visual- and somatosensory cortex (Fig. 2*A,B*). The particular shape of the STDP curves is subject to this uncertainty. However, the frequency dependence of the plasticity is dominantly dictated by the calcium time constant, τ_{Ca}, which describes the interaction time scale between consecutive spikes. This parameter is well constrained by the regular plasticity data, and in turn, the main conclusions drawn here which concern the behavior of the model for interactions between consecutive stimuli are robust.

Conclusion

By including short-term plasticity effects in a calcium-based model of long-term plasticity, we aimed here to link the different time scales at which synapses modify their strength. Both, short-term and long-term plasticity influence each other and we suggest that this interaction might be region and synapse specific. Cortical cells have a large repertoire to adapt their responses to activity- or stimulus statistics on a range of time scales such as spike-frequency adaption on the millisecond scale (Benda and Herz 2003), or homeostatic plasticity on the scale of hours (Turrigiano and Nelson 2004). Our results lend support to the idea that these mechanisms might act in a concerted fashion and that their dynamics ranges are well adjusted.

Acknowledgements

We are thankful to Srdjan Ostojic for carefully reading the manuscript and providing helpful comments.

References

Abbott, L. F. (1997, jan). Synaptic Depression and Cortical Gain Control. *Science (80-.). 275*(5297), 221–224.

Abbott, L. F. and S. B. Nelson (2000, nov). Synaptic plasticity: taming the beast. *Nat. Neurosci. 3 Suppl*(november), 1178–83.

Abbott, L. F. and W. G. Regehr (2004, oct). Synaptic computation. *Nature 431*(7010), 796–803.

Benda, J. and A. V. Herz (2003, nov). A Universal Model for Spike-Frequency Adaptation. *Neural Comput. 15*(11), 2523–2564.

Betz, W. J. (1970, mar). Depression of transmitter release at the neuromuscular junction of the frog. *J. Physiol. 206*(3), 629–644.

Bi, G. Q. and M. M. Poo (1998, dec). Synaptic modifications in cultured hippocampal neurons: dependence on spike timing, synaptic strength, and postsynaptic cell type. *J. Neurosci. 18*(24), 10464–72.

Bienenstock, E. L., L. N. Cooper, and P. W. Munro (1982, jan). Theory for the development of neuron selectivity: orientation specificity and binocular interaction in visual cortex. *J. Neurosci. 2*(1), 32–48.

Campanac, E. and D. Debanne (2008). Spike timing-dependent plasticity: a learning rule for dendritic integration in rat CA1 pyramidal neurons. *J. Physiol. 586*, 779–793.

Chung, S., X. Li, and S. B. Nelson (2002, apr). Short-term depression at thalamocortical synapses contributes to rapid adaptation of cortical sensory responses in vivo. *Neuron 34*(3), 437–446.

Crochet, S. and C. C. H. Petersen (2006, may). Correlating whisker behavior with membrane potential in barrel cortex of awake mice. *Nat. Neurosci. 9*(5), 608–610.

Dittman, J. S., A. C. Kreitzer, and W. G. Regehr (2000, feb). Interplay between facilitation, depression, and residual calcium at three presynaptic terminals. *J. Neurosci. 20*(4), 1374–1385.

Dudek, S. M. and M. F. Bear (1992, may). Homosynaptic long-term depression in area CA1 of hippocampus and effects of N-methyl-D-aspartate receptor blockade. *Proc. Natl. Acad. Sci. U. S. A. 89*(10), 4363–7.

Fernando, S. and K. Yamada (2012). Spike-timing-dependent plasticity and short-term plasticity jointly control the excitation of Hebbian plasticity without weight constraints in neural networks. *Comput. Intell. Neurosci. 2012*, 968272.

Fioravante, D. and W. G. Regehr (2011, apr). Short-term forms of presynaptic plasticity. *Curr. Opin. Neurobiol. 21*(2), 269–274.

Froemke, R., I. Tsay, M. Raad, J. Long, and Y. Dan (2006). Contribution of individual spikes in burst-induced long-term synaptic modification. *J. Neurophysiol. 95*(3), 1620.

Froemke, R. C. and Y. Dan (2002, mar). Spike-timing-dependent synaptic modification induced by natural spike trains. *Nature 416*(6879), 433–8.

Gerstner, W., R. Kempter, J. L. van Hemmen, and H. Wagner (1996, sep). A neuronal learning rule for sub-millisecond temporal coding. *Nature 383*(6595), 76–81.

Graupner, M. and N. Brunel (2010, jan). Mechanisms of induction and maintenance of spike-timing dependent plasticity in biophysical synapse models. *Front. Comput. Neurosci. 4*(September), 1–19.

Graupner, M. and N. Brunel (2012, feb). Calcium-based plasticity model explains sensitivity of synaptic changes to spike pattern, rate, and dendritic location. *Proc. Natl. Acad. Sci. U. S. A. 109*(10), 3991–3996.

Graupner, M., P. Wallisch, and S. Ostojic (2016, nov). Natural Firing Patterns Imply Low Sensitivity of Synaptic Plasticity to Spike Timing Compared with Firing Rate. *J. Neurosci. 36*(44), 11238–11258.

Hennig, M. H. (2013, apr). Theoretical models of synaptic short term plasticity. *Front. Comput. Neurosci. 7*, 45.

Higgins, D., M. Graupner, and N. Brunel (2014, oct). Memory Maintenance in Synapses with Calcium-Based Plasticity in the Presence of Background Activity. *PLoS Comput. Biol. 10*(10), e1003834.

Izhikevich, E. M. and N. S. Desai (2003, jul). Relating STDP to BCM. *Neural Comput. 15*(7), 1511–23.

Kempter, R., W. Gerstner, and J. L. van Hemmen (1999). How the threshold of a neuron determines its capacity for coincidence detection. *Biosystems. 48*(1-3), 105–12.

Kilpatrick, Z. P. (2018, may). Synaptic mechanisms of interference in working memory. *Sci. Rep. 8*(1), 7879.

Leng, L., R. Martel, O. Breitwieser, I. Bytschok, W. Senn, J. Schemmel, K. Meier, and M. A. Petrovici (2018, dec). Spiking neurons with short-Term synaptic plasticity form superior generative networks. *Sci. Rep. 8*(1), 10651.

Liley, A. W. and K. A. K. North (1953, sep). an Electrical Investigation of Effects of Repetitive Stimulation on Mammalian Neuromuscular Junction. *J. Neurophysiol. 16*(5), 509–527.

Livingstone, M. S. and D. H. Hubel (1981, jun). Effects of sleep and arousal on the processing of visual information in the cat. *Nature 291*(5816), 554–561.

Loebel, A. (2009). Multiquantal release underlies the distribution of synaptic efficacies in the neocortex. *Front. Comput. Neurosci. 3*(November), 27.

Magee, J. C. (1997, jan). A Synaptically Controlled, Associative Signal for Hebbian Plasticity in Hippocampal Neurons. *Science (80-.). 275*(5297), 209–213.

Markram, H. (1997, jan). Regulation of Synaptic Efficacy by Coincidence of Postsynaptic APs and EPSPs. *Science (80-.). 275*(5297), 213–215.

Markram, H., Y. Wang, and M. Tsodyks (1998, apr). Differential signaling via the same axon of neocortical pyramidal neurons. *Proc Natl Acad Sci U S A 95*(9), 5323–8.

Mongillo, G., O. Barak, and M. Tsodyks (2008, mar). Synaptic theory of working memory. *Science 319*(5869), 1543–6.

Morrison, A., M. Diesmann, and W. Gerstner (2008, jun). Phenomenological models of synaptic plasticity based on spike timing. *Biol. Cybern. 98*(6), 459–78.

Sabatini, B. L., T. G. Oertner, and K. Svoboda (2002, jan). The life cycle of Ca(2+) ions in dendritic spines. *Neuron 33*(3), 439–52.

Silver, I. A. (1990). Intracellular and extracellular changes of [Ca2+] in hypoxia and ischemia in rat brain in vivo. *J. Gen. Physiol. 95*(5), 837–866.

Sjöström, P. J., G. G. Turrigiano, and S. B. Nelson (2001, dec). Rate, timing, and cooperativity jointly determine cortical synaptic plasticity. *Neuron 32*(6), 1149–1164.

Sjöström, P. J., G. G. Turrigiano, and S. B. Nelson (2003, aug). Neocortical LTD via coincident activation of presynaptic NMDA and cannabinoid receptors. *Neuron 39*(4), 641–654.

Song, S., K. D. Miller, and L. F. Abbott (2000, sep). Competitive Hebbian learning through spike-timing-dependent synaptic plasticity. *Nat. Neurosci. 3*(9), 919–26.

Thomson, A. M. and J. Deuchars (1994, mar). Temporal and spatial properties of local circuits in neocortex. *Trends Neurosci. 17*(3), 119–126.

Tsodyks, M., K. Pawelzik, and H. Markram (1998, may). Neural Networks with Dynamic Synapses. *Neural Comput. 10*(4), 821–835.

Tsodyks, M. V. and H. Markram (1997, jan). The neural code between neocortical pyramidal neurons depends on neurotransmitter release probability. *Proc. Natl. Acad. Sci. U. S. A. 94*(2), 719–23.

Turrigiano, G. G. and S. B. Nelson (2004, feb). Homeostatic plasticity in the developing nervous system. *Nat. Rev. Neurosci. 5*(2), 97–107.

Varela, J. A., K. Sen, J. Gibson, J. Fost, L. F. Abbott, and S. B. Nelson (1997, oct). A quantitative description of short-term plasticity at excitatory synapses in layer 2/3 of rat primary visual cortex. *J. Neurosci. 17*(20), 7926–7940.

Wang, Y., H. Markram, P. H. Goodman, T. K. Berger, J. Ma, and P. S. Goldman-Rakic (2006, apr). Heterogeneity in the pyramidal network of the medial prefrontal cortex. *Nat. Neurosci. 9*(4), 534–542.

Zucker, R. S. and W. G. Regehr (2002, mar). Short-Term Synaptic Plasticity. *Annu. Rev. Physiol. 64*(1), 355–405.